

Short Communication

## Electrochemical Study on Corrosion Behaviors of P110 Casing Steel in a Carbon Dioxide-Saturated Oilfield Formation Water

Runcheng XIE<sup>1,2,\*</sup>, Zhanyu GU<sup>3</sup>, Yong YAO<sup>2</sup>, Hao XU<sup>2</sup>, Kun DENG<sup>2</sup>, Yi LIU<sup>2</sup>

<sup>1</sup> State Key Lab of Oil and Gas Reservoir Geology and Exploitation, Chengdu University of Technology, Chengdu 610059 China;

<sup>2</sup> College of Resources, Chengdu University of Technology, Chengdu 610059 China;

<sup>3</sup> Southwest Branch Company, SINOPEC, Chengdu 610041, China

\* E-mail: [xieruncheng@cdut.cn](mailto:xieruncheng@cdut.cn)

Received: 15 April 2015 / Accepted: 9 May 2015 / Published: 27 May 2015

---

The corrosion behaviors of P110 casing steel in a CO<sub>2</sub>-saturated oilfield formation water were investigated by electrochemical measurements and surface characterization. The corrosion resistance was obtained by weight loss method and immersion tests. The corrosion behaviors and corrosion mechanisms were investigated by using the scanning electron microscopy (SEM), energy dispersive spectrometry (EDS), open circuit potential (OCP) monitoring, polarization test and electrochemical impedance spectroscopy (EIS) techniques. The results showed that, in CO<sub>2</sub> environment, the corrosion film that formed on the P110 steel surface mainly consisted FeCO<sub>3</sub>. There was a short period with no film covering on the steel surface, due to the insufficient Fe<sup>2+</sup> concentration in the solution. As the corrosion proceeding, the concentration of Fe<sup>2+</sup> increased. When the value of [Fe<sup>2+</sup>] × [CO<sub>3</sub><sup>2-</sup>] reached high enough, FeCO<sub>3</sub> would deposit on the steel surface continuously. Therefore, a complete-covered FeCO<sub>3</sub> film formed on the steel surface, and thus the corrosion of the steel substrate was restrained.

---

**Keywords:** P110 casing steel; CO<sub>2</sub> corrosion; Corrosion resistance; Corrosion film

### 1. INTRODUCTION

Since 1970s, there have been so many pipeline failures reported around the world. In the oil and gas industry, carbon dioxide (CO<sub>2</sub>) is believed to exist in most oil and gas resources, which dissolves in water, and thus causing serious corrosion on casing steels, such as P110 carbon steel [1-5]. On the other, the CO<sub>2</sub>-enhanced oil recovery (EOR) technique has become more and more widely used in the modern petroleum industry owing to its positive contributions to the geological storage of

carbon, especially for deep wells and super deep wells [6]. Therefore, the control of the carbon dioxide corrosion has become a research hotspot recently.

For carbon steels used as casing in CO<sub>2</sub> environment, corrosion resistance is of vital importance, which has been studied by numerous researchers. A lot have reported that a protective film forms on the steel surface in CO<sub>2</sub> environment, which decreases the substrate corrosion in the later period of the corrosion process [7-10]. However, there is still no general agreement about the CO<sub>2</sub> corrosion mechanisms as a result of the multitudinous influence factors and the complexity of the chemical reaction mechanism, especially the unknown intermediates in the reactions occurred on the steel surface. For the anode reaction, one reaction was believed that the iron atom loses two electrons into bivalent iron ion, but the intermediate is still not conclusive. Presently, there is a popular conclusion which believes that this intermediate is FeOH [11,13,16,17]. However, there are still insufficient experimental proofs on this conclusion. For cathode reaction, points of view are different. In the early time, most believed that the H<sub>2</sub>CO<sub>3</sub> is reduced directly [18,19]. However, despite more than three decades of intense research, it is still unknown with absolute certainty whether H<sub>2</sub>CO<sub>3</sub> is reduced directly or the final step in the cathode reaction follows the dissociation of the H<sub>2</sub>CO<sub>3</sub>. Moreover, Gray [20] has suggested that the direct reduction of bicarbonate ion becomes dominant at higher pH level, which is due to the increasing concentration of bicarbonate with the pH increasing. A recent study also shows that pH is a key factor for the cathode reaction on the carbon steels and low alloy steels, and brings forward two critical pH values for the changing of the cathode reactions on a low alloy steel surface, which suggests that the direct reduction of HCO<sub>3</sub><sup>-</sup> was the dominant reaction at pH > 4.7, while at pH < 3.9, the direct reduction of H<sup>+</sup> was the dominant reaction [15].

In this work, a P110 carbon steel which is usually used as casing steel in oil petroleum was chosen as the experimental material. The corrosion resistance and electrochemical corrosion behaviors of this steel in a CO<sub>2</sub>-saturated oil field formation water were investigated by immersion tests, surface analysis and electrochemical techniques.

## 2. EXPERIMENTAL DETAILS

### 2.1 Materials and solutions

The experimental material was P110 casing steel. Table 1 lists the main chemical composition of P110 steel.

**Table 1.** Composition of P110 steel (wt, %)

C	Si	Mn	S	P	Cr	Mo	Ni	Ni	Ti	Cu	Fe
0.22	0.18	1.50	0.002	0.005	0.18	0.03	0.01	0.01	0.023	< 0.01	Bal.

The solution, simulating the formation water in an oil field in Southwest China, were made from analytical grade reagents and deionized water, with a chemical composition shown in Table 2.

**Table 2.** Main composition of formation water

Composition	Cl <sup>-</sup>	SO <sub>4</sub> <sup>2-</sup>	HCO <sub>3</sub> <sup>-</sup>	Na <sup>+</sup>	K <sup>+</sup>	Ca <sup>2+</sup>	Mg <sup>2+</sup>	Fe <sup>2+</sup>
Concentration mg/L	40035	10.8	714	19364	618	4787	302	338

## 2.2 Preparation of corrosion film

The immersion tests were performed to obtain the corrosion film on the P100 casing steel surface. The solution was deaerated by pouring CO<sub>2</sub> for 8 h before the test. Then the specimen was immersed into the solution. At the same time, the CO<sub>2</sub> was purged at a low flowing rate, which will ensure the saturation of CO<sub>2</sub> during the entire test. After various periods (2, 24, 72 and 120 h) of immersion, the corroded specimens were removed from the solution and rinsed with absolute ethyl alcohol.

The surface and cross-section morphologies for the corrosion film on the steel surface were observed using scanning electron microscopy (SEM) and quadrant back scattering detector (QBSD).

## 2.3 Electrochemical measurements

A three-electrode electrochemical cell was used for potentiodynamic sweeps and electrochemical impedance spectroscopy (EIS) measurements. The working electrodes (WE) were made from P110 steel. Coupons were cut into 10 mm × 10 mm × 5 mm. The unexposed faces and edges were coated with epoxy resin, and the WE had an exposed area of 1 cm<sup>2</sup>. Before each test, the working surface of WE was polished by silicon carbide sand paper to a 1000 grit grade, rinsed with deionized water, acetone and absolute ethyl alcohol successively. A platinum sheet, as a counter electrode (CE), was used in sweep and EIS tests. The surface area of the CE was 2.25 cm<sup>2</sup>, which was much larger than the surface area of working electrode (WE). A saturated calomel electrode (SCE) was connected to the cell via a Luggin capillary through a porous Vycor frit. The electrochemical tests were done using a potentiostat. In potentiodynamic sweeps, the WE was polarized from a potential of 300 mV below OCP to a potential of 300 mV. The scan rate was 0.5 mV·s<sup>-1</sup>. The impedance spectra were recorded at different time intervals using a 10 mV sinusoidal perturbing signal in the frequency range between 100 kHz and 10 mHz with six points per decade.

In all tests, the test temperature was 90 °C and the pressure was the atmospheric pressure with pure CO<sub>2</sub>.

### 3. RESULTS AND DISCUSSION

#### 3.1 Corrosion rates

As a key indicator to the evaluation of the material corrosion performance, the corrosion rates of P110 steel corroded in CO<sub>2</sub> environment were obtained by the weight loss method. Fig. 1 shows the corrosion rates for P110 casing steel after 2, 24, 72 and 120 h of immersion in the CO<sub>2</sub>-saturated oilfield formation water. It can be found that the corrosion rate for P110 steel decreased with the corrosion time increasing. At the initial corrosion period, i.e. after 2 h immersion, the corrosion rate was very high, which was up to approximately 14 mm/y. After the immersion of 24 h, the corrosion rate kept at a high level, about 12 mm/y. This was probably caused by the protective film not yet forming on the steel surface. When the immersion time reached 120 h, the corrosion rate reached a quite low value (~ 4 mm/y), which was much lower than the initial corrosion rate (14 mm/y). This was probably due to the formation of the complete-covered protective film on the steel surface. In a word, the corrosion rate of P110 steel decreased with corrosion proceeding. This was consistent with the experimental results from the other researchers [11].

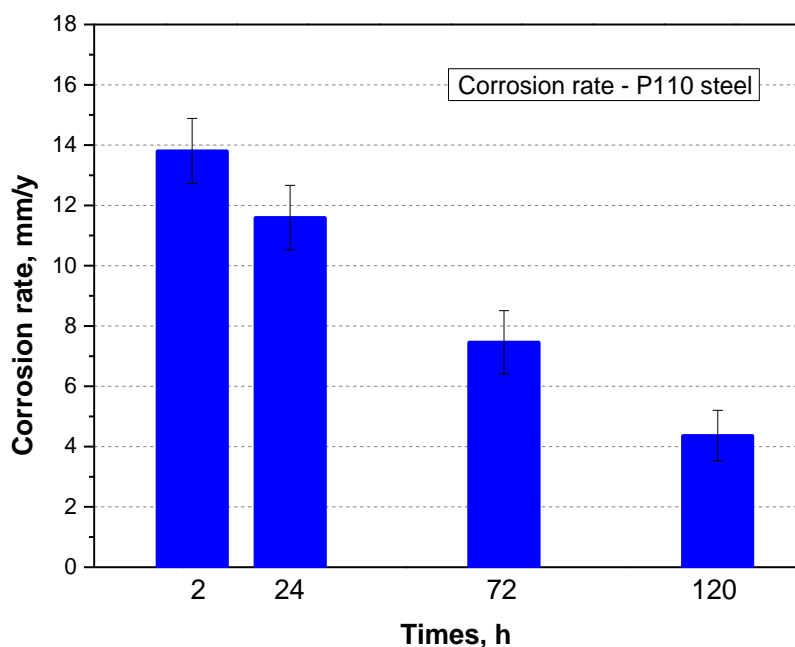


**Figure 1.** Corrosion rates for P110 casing steel in a CO<sub>2</sub>-saturated oilfield formation water

#### 3.2 Phase equilibrium of a CO<sub>2</sub>-saturated solution

Knowing the concentration of all kinds of ions in the CO<sub>2</sub> solution is of vital importance to the investigation of the corrosion performance and the corrosion mechanism for the steel. Therefore, in this section the equilibria of the CO<sub>2</sub>-saturated solution at 90 °C and 1 bar CO<sub>2</sub> pressure was obtained by a phase equilibrium mathematical model which was proposed by Zhu [15]. Fig. 2 shows the

calculating results for the phase equilibrium of a CO<sub>2</sub>-saturated solution in an open system. Overall, it can be found that the concentration of H<sub>2</sub>CO<sub>3</sub> kept constant at about 1.58×10<sup>-5</sup> mol/L as a result of the CO<sub>2</sub> continuous pouring into the solution in an open system. On the other hand, both the concentrations of HCO<sub>3</sub><sup>-</sup> and CO<sub>3</sub><sup>2-</sup> increased exponentially with the pH increasing. At pH 6, the concentration of HCO<sub>3</sub><sup>-</sup> reached about 0.224 mol/L, which was about 4 magnitude greater than that of CO<sub>3</sub><sup>2-</sup> (~ 1.66×10<sup>-5</sup> mol/L). So, it can be suggested that the direct reduction of HCO<sub>3</sub><sup>-</sup> (Eq. 1 and 2 [15]) is probably the dominant reaction during the corrosion of P110 steel under the given experimental conditions in this work.

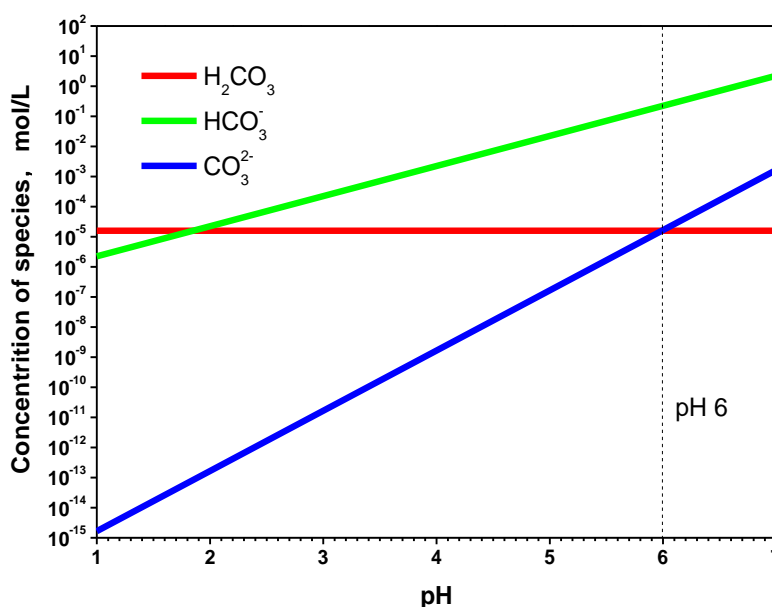
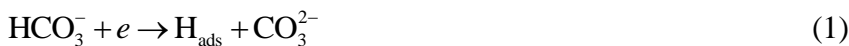


Figure 2. Equilibria of a CO<sub>2</sub>-saturated solution obtained by using Zhu’s model [15]

### 3.3 Surface and cross-section morphologies

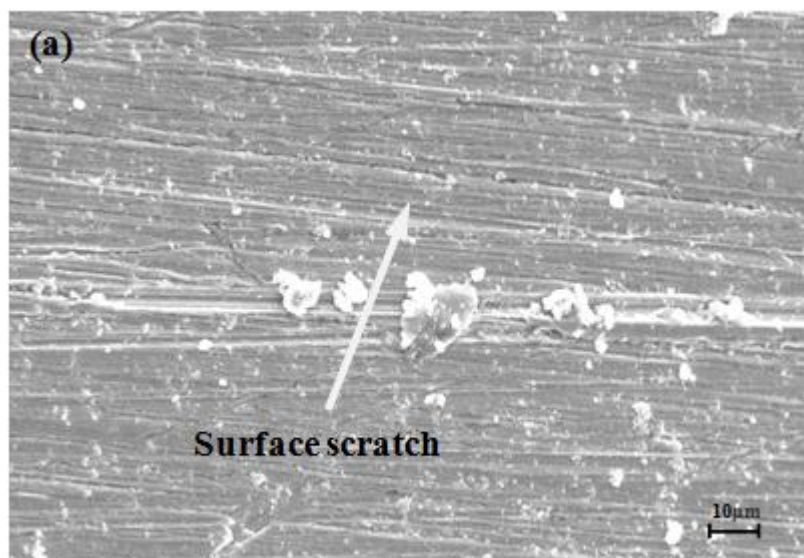
Fig. 3 shows the surface morphologies of the corrosion film that formed on the P110 steel surface with different pre-corrosion periods. In Fig. 3a, it can be seen that there was no corrosion product distributed on the steel surface, indicating that no film formed and there was a short no-film stage in the initial corrosion of P110 steel in the CO<sub>2</sub>-saturated solution. This was related to the supersaturation (SS), which was defined as the ratio of the crystallizing substance concentration to the solubility product for FeCO<sub>3</sub> (K<sub>sp</sub>) (Eq. 3). The solubility product, K<sub>sp</sub>, of FeCO<sub>3</sub> and supersaturation (SS) can be expressed [21]:

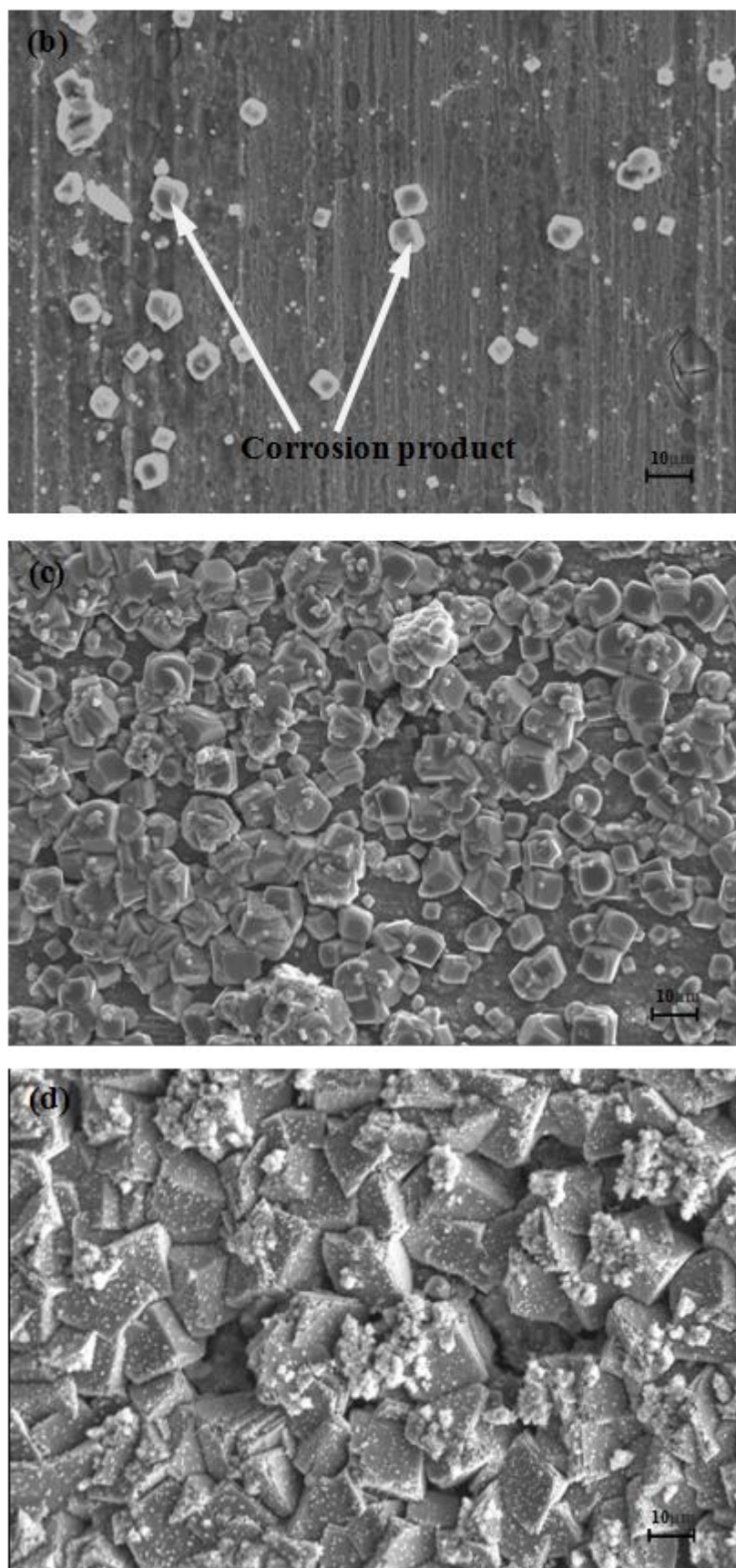
$$SS = \frac{[\text{Fe}^{2+}] \cdot [\text{CO}_3^{2-}]}{K_{\text{sp}}} \tag{3}$$

As the corrosion period increasing, the concentration of  $\text{Fe}^{2+}$  in the solution increased. Only when the product of  $[\text{Fe}^{2+}]$  and  $[\text{CO}_3^{2-}]$  exceeds  $K_{\text{sp}}$  of  $\text{FeCO}_3$  (i.e.  $SS > 1$ ), can  $\text{FeCO}_3$  begin to nucleate and deposit on the steel surface. Therefore, the initial stage of the corrosion had a no-film period. This is also the reason why that the initial corrosion rate of P110 steel in Fig. 1 was so high. The bare steel without any protective covering could dissolve quickly and therefore exhibited a very high corrosion rate, about 14 mm/y at 0.2 h (see Fig. 1).

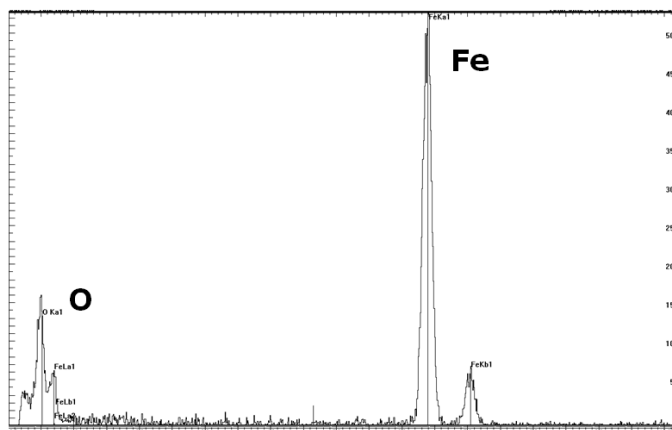
After 24 h of immersion, as shown in Fig. 3b, some cubic particles with size of about 5-10  $\mu\text{m}$  were distributed on the steel surface due to the  $\text{Fe}^{2+}$  concentration increasing with the corrosion proceeding. A lot previous researchers have proposed that these particles were mainly composed of  $\text{FeCO}_3$ . In order to confirm this statement, the energy dispersive spectrometry (EDS) measurement was conducted on the particles in Fig. 3b. As shown in Fig. 4, two clearly peaks corresponding to O and Fe were observed in the EDS spectrum. The C element was not able to be detected in the EDS test. Also, the O/Fe ratio was near to 3, indicating that the particles formed on the steel surface probably contained  $\text{FeCO}_3$ , which was consistent with the results from the previous studies. Although corrosion product began to form on the steel surface, the amount was too small. Therefore, these scattered particles of corrosion product were not able to protect the steel substrate effectively, and the corrosion rate of the steel still kept at a high level ( $\sim 12$  mm/y).

Fig. 3c and Fig. 3d show the SEM photos of the corrosion film that formed on the steel surface after 72 and 120 h of immersion, respectively. Obviously, there were much more corrosion products that covered on the steel surface in Fig. 3c and d than those in Fig. 3a and b. With corrosion period increasing, the  $\text{Fe}^{2+}$  concentration increased due to the continuous corrosion of the substrate. Therefore, the  $\text{Fe}^{2+}$  and  $\text{CO}_3^{2-}$  combined and  $\text{FeCO}_3$  deposited on the steel surface continuously. In this way, a much denser corrosion film formed, and the corrosion rate decreased. At 120 h, the corrosion rate fell to about 4 mm/y as shown in Fig. 1. On the other hand, the  $\text{FeCO}_3$  particles in Fig. 3d were much bigger than those in Fig. 3c. At 120 h, the grain size of the  $\text{FeCO}_3$  particles reached approximately 15~20  $\mu\text{m}$ , which was about two times larger than that of 72 h. This was related to the growing of the crystals with the corrosion proceeding.



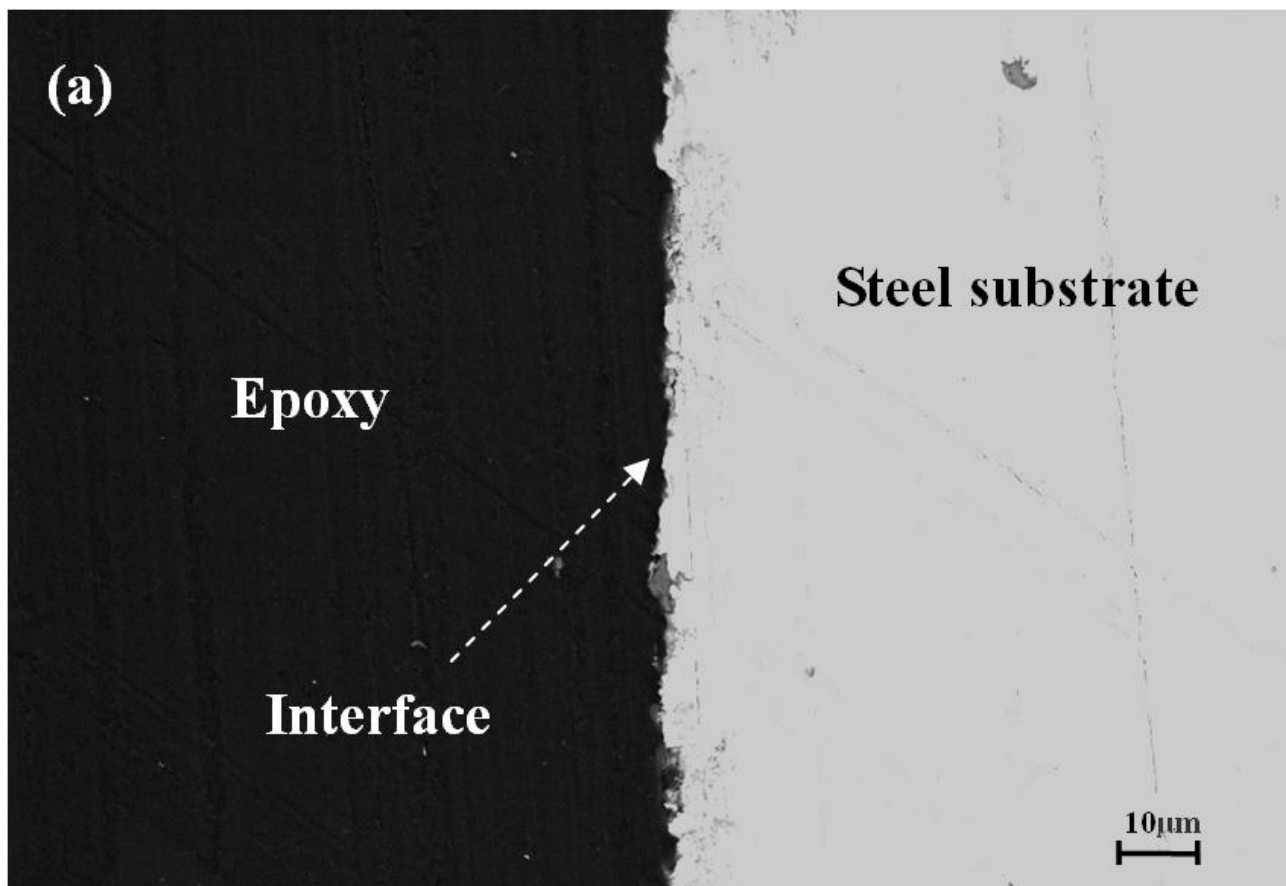


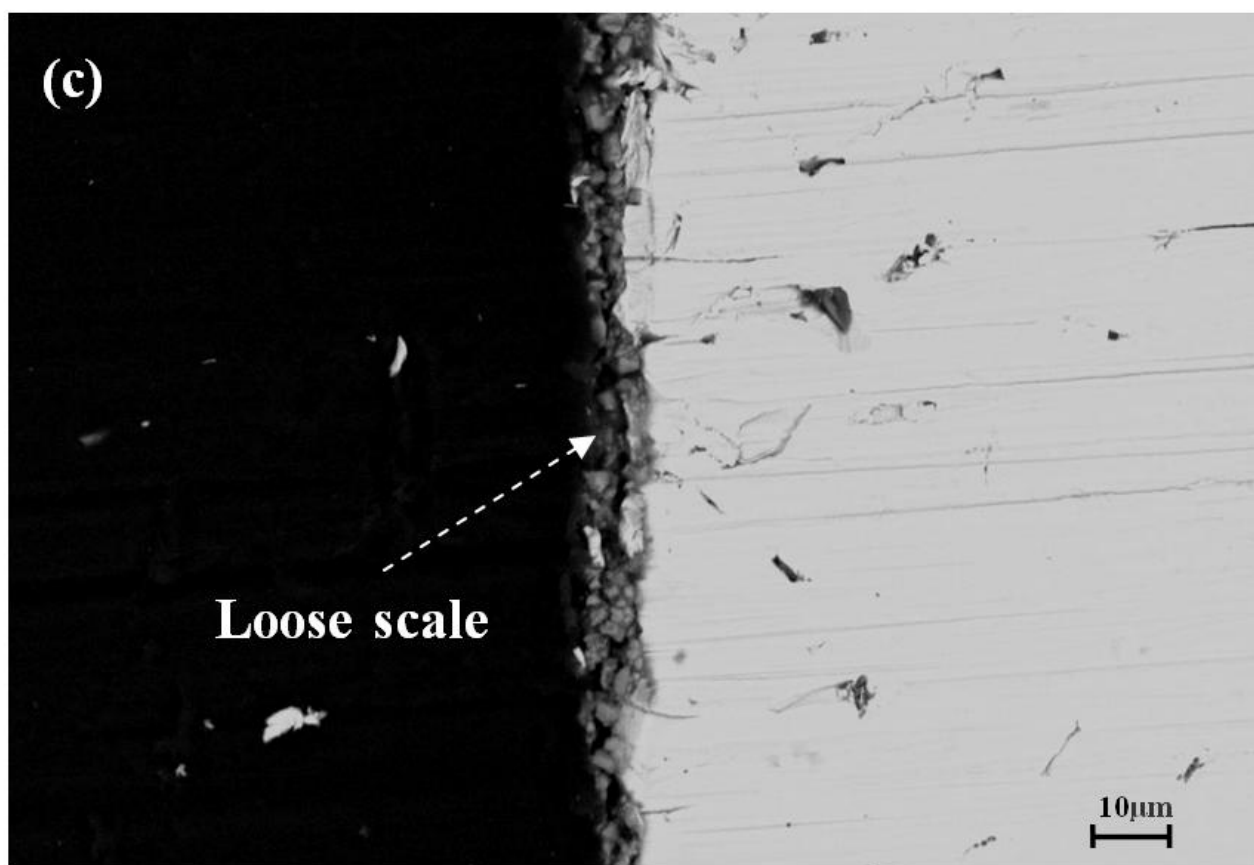
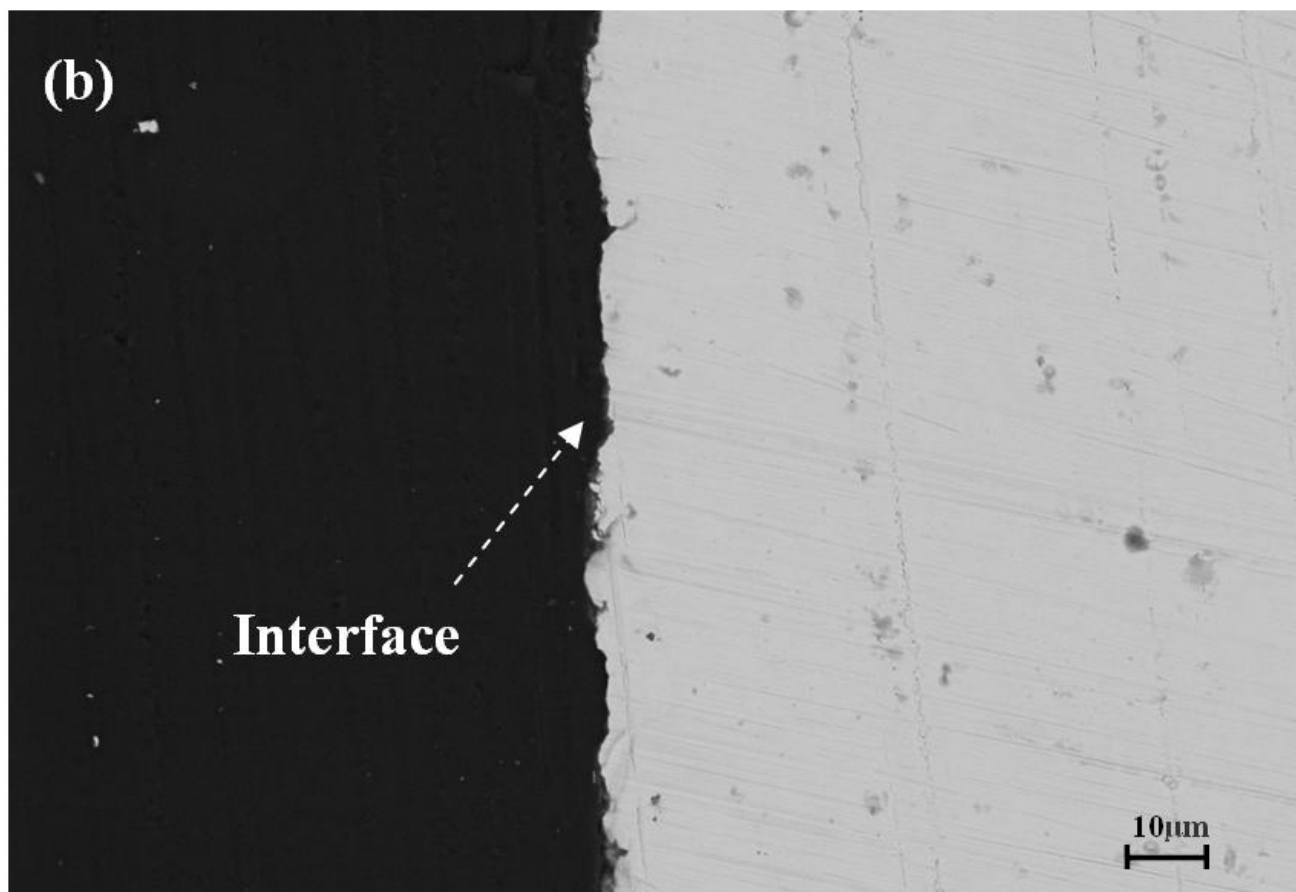
**Figure 3.** Surface morphologies of corrosion films formed on P110 steel with various immersion times: (a) 2 h; (b) 24 h; (c) 72 h; (d) 120 h



**Figure 4.** EDS results for the corrosion product on the P110 steel surface after 24 h immersion

Fig. 5a-d show the cross-sectional morphologies of the corrosion films that formed on P110 casing steel after 2, 24, 72 and 120 h, respectively. It can be seen that no film was observed on the steel surface in Fig. 5a and b. After 24 h of immersion, a looser film with about 5~8 μm thickness was observed on the steel surface (Fig. 5c). When the corrosion period reached 120 h, the film became much thicker (about 20~30 μm) and denser, which was due to the continuous nucleation and growth of the corrosion product on the steel surface (Fig. 5d). This was consistent with the results in Fig. 3.





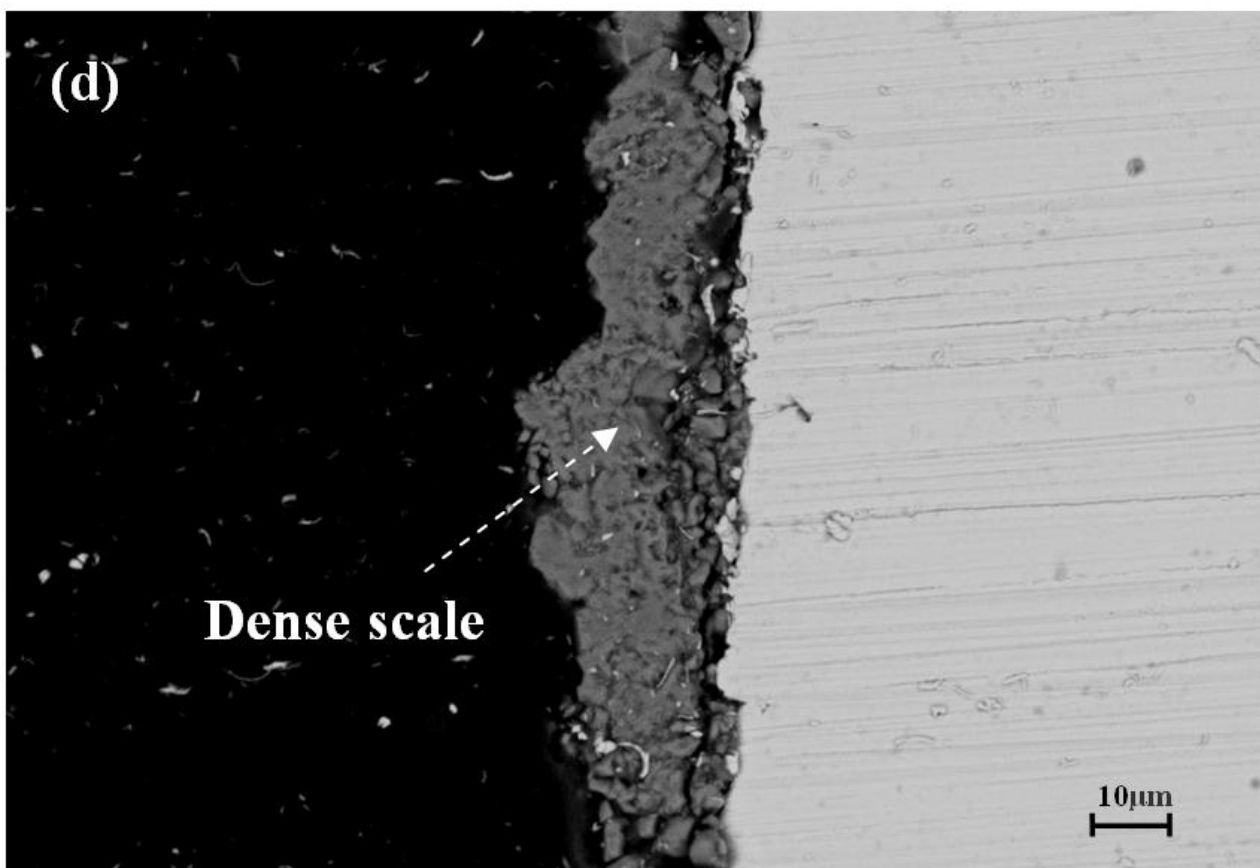


**Figure 5.** Cross-section morphologies of corrosion films formed on P110 steel with various immersion times: (a) 2 h; (b) 24 h; (c) 72 h; (d) 120 h

### 3.3 Electrochemical measurements

The open circuit potential (OCP) monitoring is very important to the investigation of the corrosion behaviors and corrosion proceeding analysis for the steel. Fig. 6 shows the OCP values changing with the corrosion time for P110 steel in a CO<sub>2</sub>-saturated oilfield formation water. It can be found that the OCP values changed with time and tend to be steady after a certain period of the immersion. About before 150 s, the OCP values kept increase with the increasing of the time, which increased from -718 mV to -711 mV (vs. SCE, the same below). After that, the OCP values tended to be steady, and fluctuated between -710 mV and -712 mV. Then, when the OCP values were steady, the potentiodynamic polarization measurement was conducted on the electrode surface. Fig. 7 gives the potentiodynamic polarization curve for the P110 steel corroded in CO<sub>2</sub> environments. For the cathode domain, the curve was much straighter than that in the anode region. For anode domain, no passivation behavior was observed and the corrosion current density always increased with the applied potential increasing. This was probably related to the lower pH values in the CO<sub>2</sub> solutions. In our given solution, the pH was 6, which was not alkaline enough to make the steel in passivation. Therefore, the steel in our given environment corroded seriously and the corrosion rate was very high during the initial corrosion period.

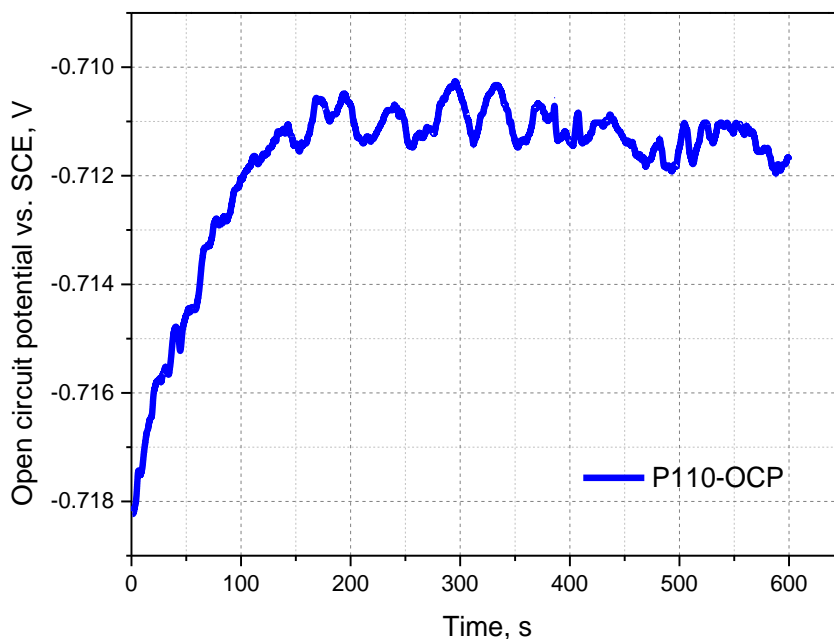


**Figure 6.** Open circuit potential monitoring result for the P110 steel corroded in a CO<sub>2</sub>-saturated solution

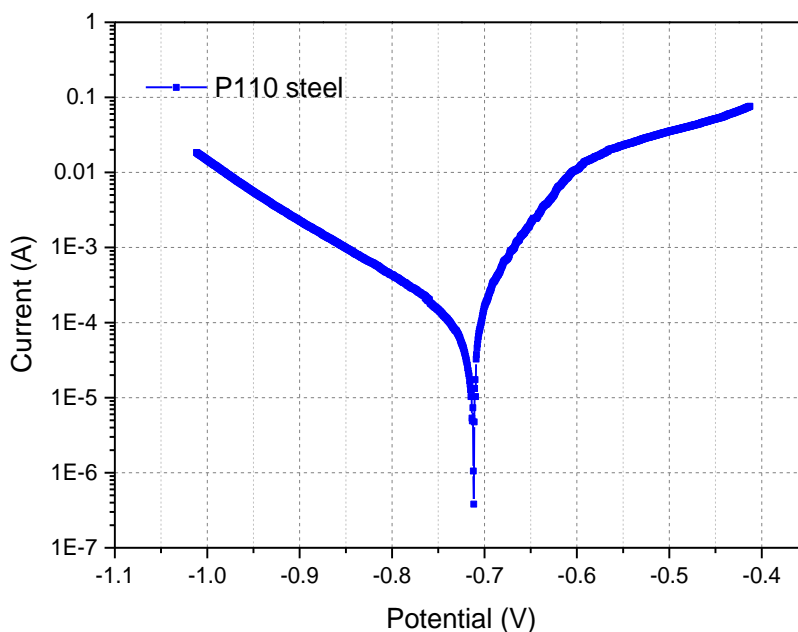


**Figure 7.** Potentiodynamic polarization curves of X60 and Cr2Ni steels.

It is well known that the corrosion rate measurements illustrate the evolution of the dissolution of the steel surface under the given environment in this work. Electrochemical impedance spectroscopy (EIS) measurements can provide insight into the corrosion mechanisms occurring at the

interface. Therefore, to give a deeper investigation on the growth of the corrosion film and corrosion mechanism for the P110 steel in the CO<sub>2</sub>-saturated solution, the EIS measurements were performed in this section. Fig. 8, Fig. 9 and Fig. 10 show the Nyquist diagrams for the P110 steel after the immersion of 2, 72 and 120 h in a CO<sub>2</sub>-saturated oilfield formation water, respectively. It is seen that, as shown in Fig. 7, after 2 h of immersion the impedance spectra exhibited a capacitive semicircle in the high frequency range and an inductive loop in the low frequency range. The inductive loop in the low frequency range was probably related to the adsorption of the intermediate product [22,23]. After 72 h of immersion, the high frequency capacitive semicircle increased and the low frequency inductive loop shrank. This was contributed to the formation of the FeCO<sub>3</sub> film on the steel surface. As shown in Fig. 3c, a film has formed and covered on the steel surface, which protected the substrate from the further corrosion, thus the capacitive semicircle increased. However, this film was not complete-covered. Therefore, the inductive loop still existed and shrank. At 120 h, the impedance spectrum was consisted of two capacitive semicircles, indicating that a complete-covered film formed, which is consistent with the SEM result in Fig. 3d. Moreover, the semicircle increased significantly at 120 h, corresponding to the lowest corrosion rate in this stage.

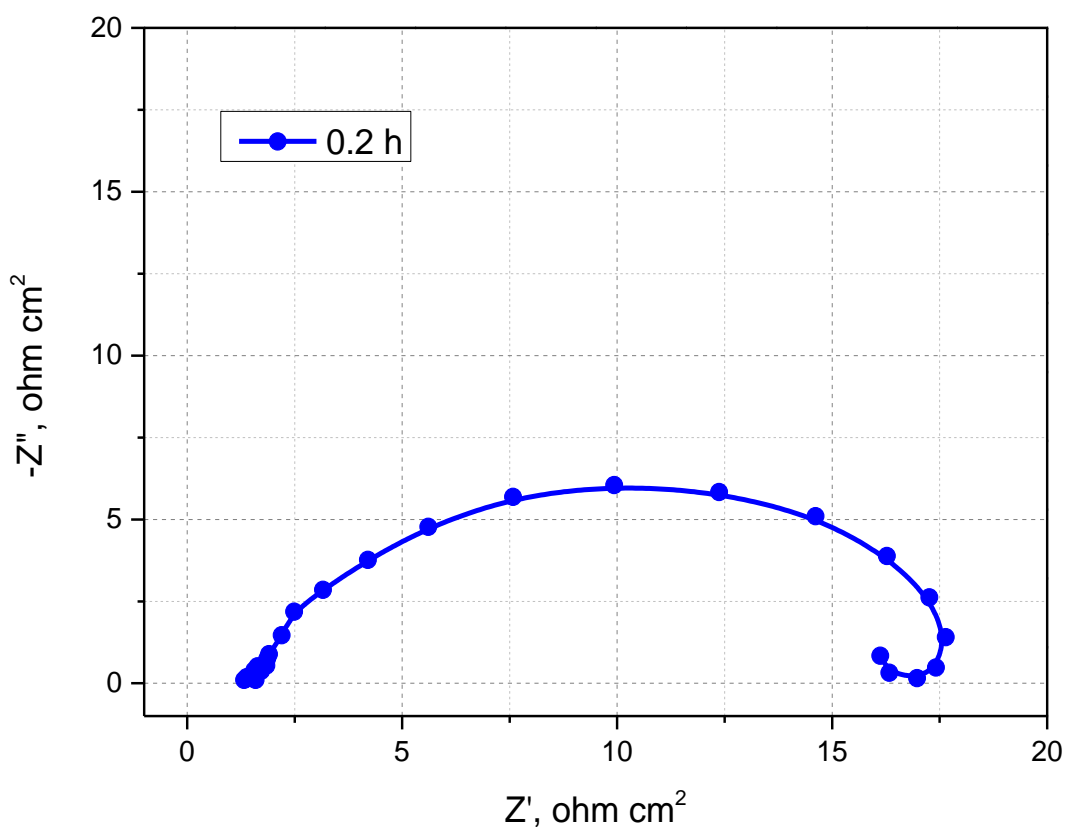


**Figure 8.** Nyquist diagram for P110 steel in the CO<sub>2</sub>-saturated solution obtained after the immersion of 2 h.

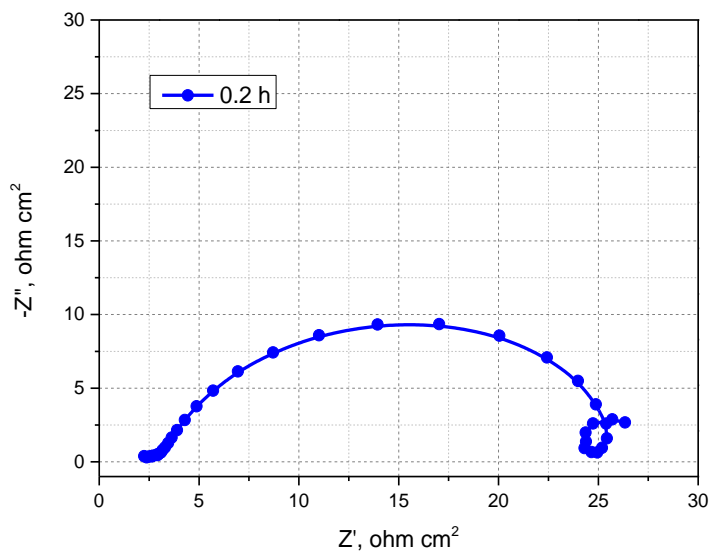


**Figure 9.** Nyquist diagram for P110 steel in the CO<sub>2</sub>-saturated solution obtained after the immersion of 48 h.

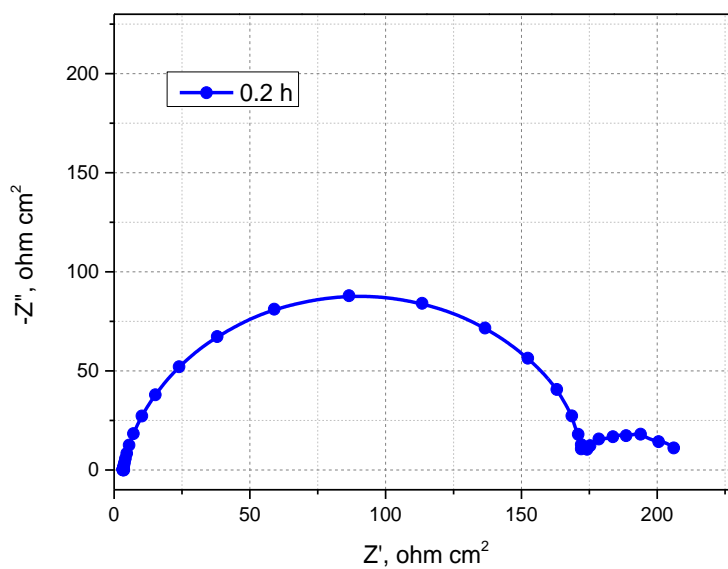


**Figure 10.** Nyquist diagram for P110 steel in the CO<sub>2</sub>-saturated solution obtained after the immersion of 120 h.

#### 4. CONCLUSION

The main conclusions which can be drawn from this study are:

- In a CO<sub>2</sub>-saturated oilfield formation water, the corrosion rate of P110 steel was very high at the initial corrosion stage. It decreased sharply when a FeCO<sub>3</sub> film of good protectiveness formed on the steel surface.
- The SEM results indicate that a short no-film period existed during the initial corrosion

of P110 steel, due to the insufficient  $\text{Fe}^{2+}$  concentration. After 24 h of immersion, the corrosion product ( $\text{FeCO}_3$ ) began to deposit on the steel surface. As the corrosion proceeding, a complete-covered film formed at last, which protected the steel substrate from the further corrosion.

#### ACKNOWLEDGMENTS

The work is funded by National Postdoctoral Science Foundation Project of the People's Republic of China under Contract No. 20110491740 and the authors acknowledge the assistance.

#### References

1. J. Y. Zhu, L. N. Xu, M. X. Lu, L. Zhang, W. Chang and L. H. Hu, *Corrosion Science*, 93 (2015) 336
2. M. B. Kerman, A. Morshed, *Corrosion*, 59 (2003) 659
3. A. Ikeda, M. Ueda, S. Muka, *Corrosion*, 39 (1983) 131
4. G. Schmitt, *Corrosion*, 3 (1984) 43
5. J. Y. Zhu, L. N. Xu, W. Chang, L. H. Hu and M. X. Lu, *Materials and Design*, 53 (2014) 405
6. J. Y. Zhu, L. N. Xu, M. X. Lu, L. Zhang and W. Chang, *RSC Advances*, 5 (2015) 18518
7. F. Yu, K. W. Gao and Y. J. Su, *Materials Letters*, 59 (2005) 1709
8. C. A. Palacios, J. R. Shadley, *Corrosion*, 47 (1991) 122
9. E. Dayalan, F. D. De Moraes and J. R. Shadley, CORROSION 98. NACE International, 1998
10. A. Dugstad, CORROSION 98. NACE International, 1998.
11. S. Netic, *Corrosion Science*, 49 (2007) 4308
12. R. W. Revie, *Corrosion and corrosion control*. John Wiley & Sons, 2008
13. B. R. Linter, G. T. Burstein, *Corrosion Science*, 41 (1999) 117
14. L. S. Moiseeva, N. S. Rashevskaya, *Russian Journal of Applied Chemistry*, 75 (2002) 1625
15. J. Y. Zhu, L. N. Xu, M. X. Lu, L. Zhang, W. Chang and L. H. Hu, *International Journal of Electrochemical Science*, 10 (2015) 1434
16. S. Netic, J. Postlethwaite and M. Vrhovac,  $\text{CO}_2$  corrosion of carbon steel-from mechanistic to empirical modeling. (1997) 211
17. F. F. Eliyan, E. S. Mahdi and A. Alfantazi, *Corrosion Science*, 58 (2012) 181
18. C. de Waard, D. E. Milliams, *Corrosion* 31 (1975) 131
19. L. G. S. Gray, B. G. Anderson, M. J. Danysh and P. G. Tremaine, CORROSION 89. NACE International, 1989
20. L. G. S. Gray, B. G. Anderson, M. J. Danysh and P. G. Tremaine, CORROSION 90. NACE International, 1990
21. E. W. J. Hunnik, B. F. M. Pots and E. L. J. A. Hendriksen, CORROSION 96. NACE International, 1996
22. J. Y. Zhu, L. N. Xu, L. M. X. Lu. *Corrosion*, 2015. doi: <http://dx.doi.org/10.5006/1494>
23. C. F. Chen, M. X. Lu, D. B. Sun, Z. H. Zhang and W. Chang, *Corrosion*, 61 (2005) 594